ORIGINAL ARTICLES

CORRELATION OF SPECTROSCOPIC AND STRUCTURAL PROPERTIES OF INDOCYANINE GREEN J-AGGREGATES

Farrakhova D.S.[1], Romanishkin I.D.[1], Yakovlev D.V.[1,2], Maklygina Yu.S.[1], Oleinikov V.A.[2], Fedotov P.V.[1,3], Kravchik M.V.[4], Bezdetnaya L.[5,6], Loschenov V.B.[1]
[1]Prokhorov General Physics Institute of the Russian Academy of Science, Moscow, Russia
[2]Shemyakin–Ovchinnikov Institute of Bioorganic Chemistry of the Russian Academy of Science, Moscow, Russia
[3]Moscow Institute of Physics and Technology, Dolgoprudny, Russia
[4]Research Institute of Eye Diseases, Moscow, Russia
[5]Institut de Cancèrologie de Lorraine, Vandoeuvre-lès-Nancy, France
[6]Centre de Recherche en Automatique de Nancy, CNRS, Universitè de Lorraine, Nancy, France

Abstract

Indocyanine green (ICG), when in free form in a liquid, can form stable nanoparticle structures or colloidal solution, while changing its spectroscopic properties. In the work, the aggregation degree and the average size of nanoparticles depending on the concentration of a colloidal solution of indocyanine green (ICG NPs) in the form of J-aggregates were investigated by various methods based on light scattering. The size of nanoparticles is an important parameter from the point of view of clinical application, because the technique of intravenous administration of drugs, in order to avoid microvascular thrombosis and embolism, provides dosage forms with inclusions of individual molecules or their clusters, not exceeding 500 nm diameter. In turn, small nanoparticles less than 30 nm lead to prolonged circulation of the drug in the body with an increased possibility of permeation into cells of healthy tissue. In the course of studies, it was found that an increase in the concentration of ICG NPs in the solution leads to an increase in the average size of spontaneously formed J-aggregates, which, in turn, leads to a decrease in the absorption coefficient in the aggregates. Presumably, this phenomenon, i.e. the established nonlinear dependence of the J-aggregate absorption on its size, can be explained by the formation of absorption centers on the J-aggregate surface in the form of mobile surface molecules. The threshold range of ICG molecule concentration was determined, at which there is a transition from aggregation with an increase in size with a slow addition of ICG J-aggregate molecules in height to a rapid addition in width.

Key words: Mie scattering, dynamic light scattering, indocyanine green, colloidal solution, J-aggregates, scattering indicatrix, aggregation degree.

For citations: Farrakhova D.S., Romanishkin I.D., Yakovlev D.V., Maklygina Yu.S., Oleinikov V.A., Fedotov P.V., Kravchik M.V., Bezdetnaya L., Loschenov V.B. Correlation of spectroscopic and structural properties of indocyanine green J-aggregates, *Biomedical Photonics*, 2022, vol. 11, no. 3, pp. 4–16. doi: 10.24931/2413–9432–2022–11-3-4–16.

Contacts: Farrakhova D.S., e-mail: farrakhova.dina@mail.ru

ВЗАИМОСВЯЗЬ СПЕКТРОСКОПИЧЕСКИХ И СТРУКТУРНЫХ СВОЙСТВ J-АГРЕГАТОВ ИНДОЦИАНИНА ЗЕЛЕНОГО

Д.С. Фаррахова[1], И.Д. Романишкин[1], Д.В. Яковлев[1,2], Ю.С. Маклыгина[1], В.А. Олейников[2], П.В. Федотов[1,3], М.В. Кравчик[4], Л. Бездетная[5,6], В.Б. Лощенов[1]
[1]Институт общей физики им. А.М. Прохорова Российской академии наук, Москва, Россия
[2]Институт биоорганической химии им. академиков М.М. Шемякина и Ю.А. Овчинникова Российской академии наук, Москва, Россия
[3]Московский физико-технический институт, Долгопрудный, Россия
[4]Научно-исследовательский институт глазных болезней им. М.М. Краснова, Москва, Россия
[5]Институт рака Лотарингии, Вандевр-ле-Нанси, Франция
[6]Центр автоматических исследований в Нанси, CNRS, Университет Лотарингии, Нанси, Франция

Резюме

Индоцианин зеленый (ICG), находясь в растворе, способен образовывать стабильные структуры наночастиц или коллоидный раствор, изменяя при этом свои спектроскопические свойства. В работе различными методами, основанными на светорассеянии, были исследованы степень агрегации и средний размер наночастиц в зависимости от концентрации коллоидного раствора наночастиц индоцианина зеленого (ICG NPs) в форме J-агрегатов. Размер наночастиц представляет собой важный параметр с точки зрения клинического применения, так как техника внутривенного введения препаратов, с целью избежания тромбозов микрососудов и эмболии, предусматривает лекарственные формы с включениями, в виде отдельных молекул или их кластеров, не превышающими в диаметре 500 нм. С другой стороны, наночастицы размером менее 30 нм длительно циркулируют в организме и могут проникать в клетки здоровой ткани. В ходе исследований, было установлено, что увеличение концентрации ICG NPs в растворе ведет к увеличению среднего размера спонтанно формируемых J-агрегатов, что в свою очередь ведет к уменьшению коэффициента поглощения в агрегатах. Предположительно, нелинейная зависимость поглощения J-агрегата от его размера, может быть объяснен формированием центров поглощения на поверхности J-агрегата в виде подвижных поверхностных молекул. Был определен пороговый диапазон концентрации молекул ICG, при котором происходит переход от агрегации с увеличением размера с медленным прибавлением молекул J-агрегата ICG в высоту, но с быстрым прибавлением в ширину.

Ключевые слова: рассеяние Ми, динамическое рассеяние света, индоцианин зеленый, коллоидный раствор, J-агрегаты, индикатриса рассеяния, степень агрегации.

Для цитирования: Фаррахова Д.С., Романишкин И.Д., Яковлев Д.В., Маклыгина Ю.С., Олейников В.А., Федотов П.В., Кравчик М.В., Бездетная Л., Лощенов В.Б. Взаимосвязь спектроскопических и структурных свойств j-агрегатов индоцианина зеленого // Biomedical Photonics. – 2022. – Т. 11, № 3. – С. 4–16. doi: 10.24931/2413–9432–2022–11-3-4–16.

Контакты: Фаррахова Д.С., e-mail: farrakhova.dina@mail.ru

Introduction

The fluorescent dye ICG is the only drug with an absorption peak in the near infrared range (NIR), approved for clinical application in most countries of the world [1]. The ICG aqueous solution consists of monomers and H-type dimers with two absorption peaks at 780 and 715 nm, respectively (Fig.1a). ICG is able to form J-aggregates under certain temperature conditions, representing a stable colloid with aggregated nanoparticles (ICG NPs) at high concentrations [2-4]. ICG J- aggregates have an absorption and fluorescence peaks in the NIR range (0,75–1,4 μm) within the biological transparency window [5], which is promising for fluorescent diagnostics [1, 6]. The formation of J-aggregates occurs due to hydrophobic, non-covalent π-π interactions between ICG molecules [3]. In this case, the dipole moments of the electronic transitions of individual molecules are practically aligned parallel to the line connecting their centers through the «head to tail» arrangement (Fig.1b) [3].

The J-aggregates in the ICG NPs colloidal solution have strong changes in spectroscopic properties, such as a narrow J-band in the absorption spectrum and its sharp shift of about 100 nm into NIR. Also, the fluorescence maximum of J-aggregates in a ICG NPs colloidal solution coincides with their absorption peak and demonstrates a behavior close to resonance, at which point, it has a small Stokes shift and insensitivity to the environment [7]. Our studies of ICG NPs colloidal solution have shown their promise for diagnostics of malignant neoplasms, as they increase the circulation of ICG monomers and

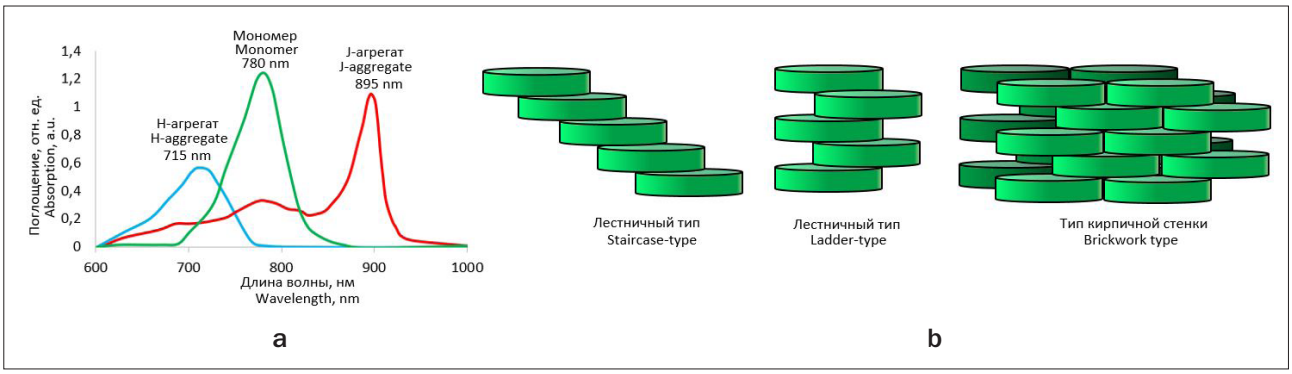

Рис. 1.
a – спектры поглощения ICG;
b – схематическая иллюстрация образования структур J-агрегатов.
Fig. 1.
a – absorption spectra of ICG;
b – schematic illustration of J-aggregate formation.

H-aggregates from 30 min to 2 days [8, 9]. Moreover, when ICG NPs interact with the environment of plasma proteins after intravenous injection, the nanoparticles demonstrate their stability, which can improve fluorescence diagnostics by increasing the circulation of the ICG monomer in the blood system, which makes it possible to predict the pathways of metastasis [10]. Based on experimental data, the determination of the optical characteristic changes of the ICG NPs colloidal solution in the tumor microenvironment remains relevant. In study [11], it was suggested that the nonlinearity of optical characteristics arises due to a decrease in the specific surface of aggregates. However, no assumption was made about the geometric alignment of the J-aggregate nanostructures and the presence of changes (inflection points) in the graphs of the absorption dependence on the concentration.

Materials and methods

The molecular form of ICG, consisting of a diluted polycrystalline powder Pulsion® (Pulsion Medical Systems, Germany), was heated in water to 65°C, and then kept at this temperature for 20 hours to form ICG NPs in accordance with the previously published method [12]. After the formation of J-aggregates, the solution was filtered through syringe filters with 0.40 μm diameter pores to remove large aggregates. A sample with 0.25 μM concentration was selected to study the spectroscopic properties of the ICG NPs colloidal solution. Polylatex calibration spheres with 110 nm diameter were used as a reference sample.

Fluorescence excitation spectra and fluorescence spectral maps were obtained via the Jobin-Yvon NanoLog-4 system (Horiba, Japan). An InGaAs charge-coupled device with 800-1600 nm operating optical range was used as a detector. A xenon lamp (operating range 300-900 nm) with a dual monochromator and 2 nm spectral resolution was used as an excitation source.

Resonant fluorescence registration experiments of ICG NPs colloidal solution were carried out by excitation of the different wavelengths in the 880-915 nm range via Chameleon Ultra II titanium-sapphire laser (Coherent, USA) with 80 MHz frequency and a 140 fs pulse length. For these studies, an installation with a spectrometer and continuous-wave laser was assembled (Fig. 2).

Laser radiation in the 880-915 nm wavelength range with a 1 nm step, passes through a focon into fiber-optic bundle, then through a vertically oriented linear polarizer onto the sample. The scattered laser radiation from the sample passes at 90° angle through a horizontally oriented linear polarizer and an optical fiber into a spectrometer. The crossed polarizer configuration makes possible to exclude the direct laser radiation. 880/10 nm narrow-band filter was also installed in front of the sample to suppress laser radiation (Fig. 2).

For obtaining the scattering indicatrix of the ICG NPs colloidal solution, an installation was assembled on a rotating platform with a receiving optical fiber and fixed optical bundle for delivering laser radiation (Fig. 3). 920 nm wavelength was chosen as laser radiation, for the reason that ICG NPs has no absorbing properties at the wavelength.

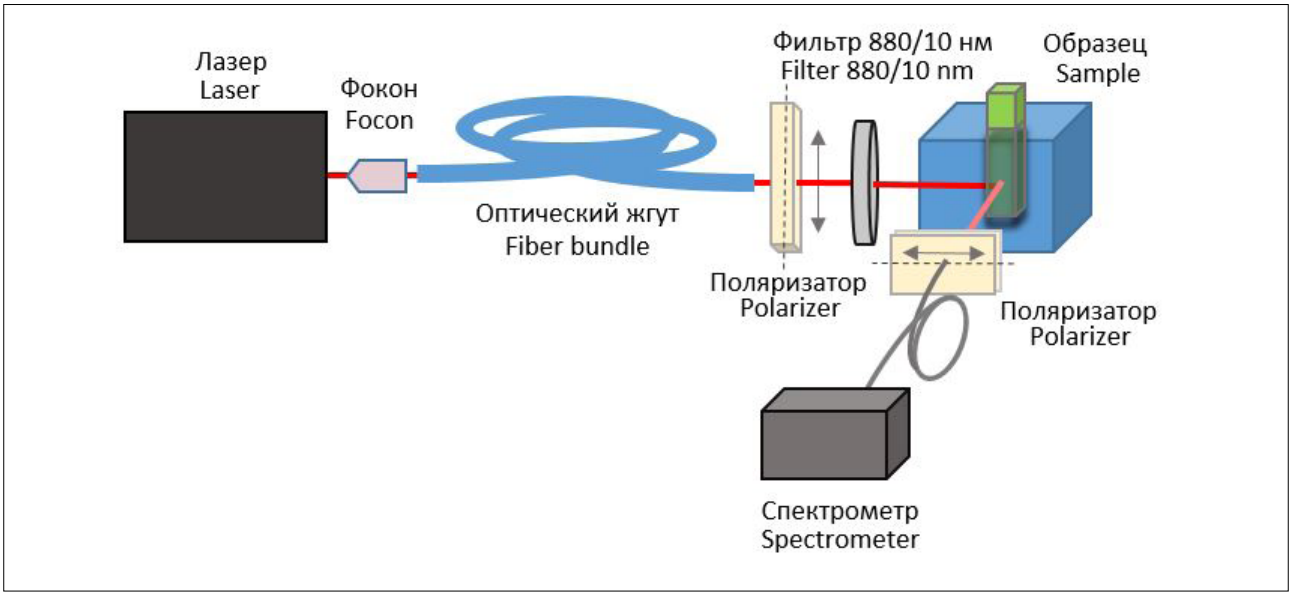

Рис. 2. Схема установки для определения спектроскопических свойств J-агрегатов ICG NPs и калибровочных сфер методом рассеяния света.
Fig. 2. Installation scheme for determination of spectroscopic properties of ICG NPs J-aggregates and calibration spheres by light scattering method.

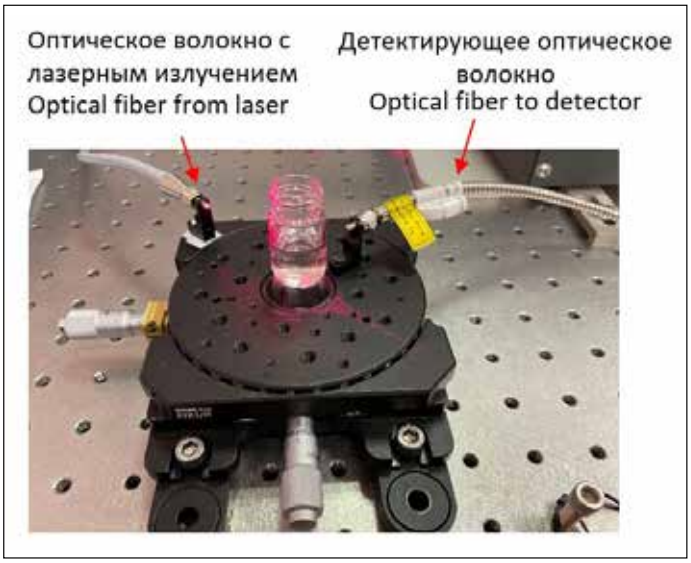

Рис. 3. Экспериментальная установка для определения индикатрисы рассеяния излучения, прошедшего через коллоидный раствор ICG NPs и образца, содержащего калибровочные сферы.
Fig. 3. Experimental installation for determining the scattering indicatrix of radiation passed through the colloidal solution of ICG NPs and the sample containing calibration spheres.

The experimental results were approximated by Henyey–Greenstein function to calculate the anisotropy factor:

$$p(cos\theta) = \frac{1-g^2}{2\left(1+g^2-2g*cos\theta\right)^{3/2}}, \quad (1)$$

where p – phase scattering function, θ – deflection angle of scattered light, g – anisotropy factor.

In the decomposition of the Henyey–Greenstein function by Legendre polynomials, the anisotropy factor is related to the expansion coefficients through the relation:

$$x_i = (2i+1)g^i, \quad (2)$$

The elongation of the scattering indicatrix is determined by this parameter.

To study the aggregate size and the aggregation degree of ICG molecules at different concentrations of ICG NPs colloidal solution, a multi-angle dynamic light scattering analyzer Photocor Complex (Photocor, Russia) was used. A He–Ne laser with 632.8 nm wavelength was used as an excitation source. 15° and 145° angles were selected to measure the power of the scattered signal on the samples of ICG NPs colloidal solution (Fig. 4).

The aggregation degree β_m demonstrates the ranking index of ICG molecules in a aggregate and is determined by comparing the scattering efficiency with the calculations of Mie scattering. The aggregation degree can be represented in the forms:

$$\beta_m = N_m / N_{ag}, \quad (3)$$

where N_m – numerical density of ICG molecules, N_{ag} – numerical density of J-aggregates, and

$$\beta_m = \frac{f_{ag} S_{ag} N_m}{a_{ag}}, \quad (4)$$

where f_{ag} – the proportionality factor**,** also called J-aggregate absorption strength, S_{ag} – absorption cross section of aggregate, a_{ag} – average size of aggregate.

Differential cross-sections of Mie scattering at different angles of light scattering on the sample were calculated to obtain the values of the aggregation degree of ICG molecules. These values were then used to calculate the average size of aggregates at different concentrations. A detailed description of the experiment

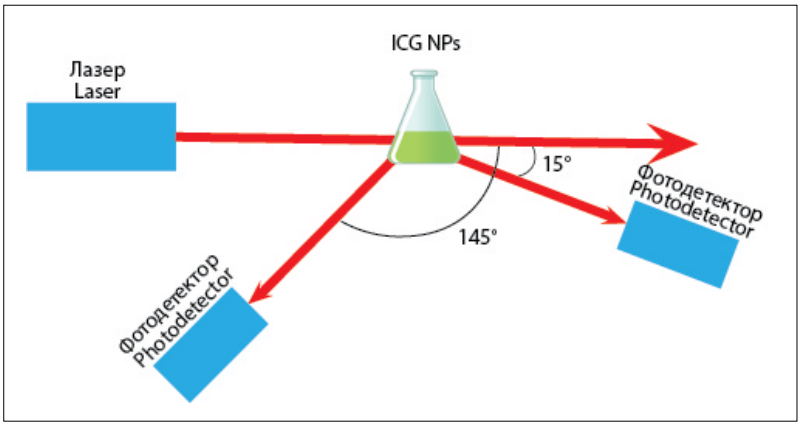

Рис. 4. Схема эксперимента измерения размера частиц методом рассеяния Ми.
Fig. 4. Experimental scheme of measuring the particle size by the Mie scattering method.

design and the theoretical derivation of the formulas are presented in work [11].

ICG NPs colloidal solution was examined by scanning electron microscopy (SEM) to study the morphological structure of J-aggregates. Before the study, samples of ICG NPs colloidal solution were frozen at 77 K (by immersion in liquid nitrogen). This method of samples temperature lowering was necessary to avoid aggregates sticking together and/or rearranging self-assembly. The pre-frozen sample was placed on the Peltier table (thermoelectric cooling) and placed in the chamber of the electron microscope EVO LS10 (Zeiss, Germany). The surface of the Peltier table was stabilized at 253 K temperature, the pressure in the chamber was 70 Pa. The Peltier table was heated from 77 K to 253 K in order to ensure the invariance of the component structure of ICG NPs samples. To avoid water screening, the surface of the ICG NPs sample droplets were subjected to preliminary electron beam effects until the structured image appeared. Observations were carried out in low vacuum mode at an 21 kV accelerating voltage and a current on the sample of 30 pA via a backscattered electron detector using a working segment of 13-13.5 mm. 1024×768 px images were recorded with 7.7 nm/px hardware resolution.

Results

The sample was irradiated with 650, 700, 750 and 800 nm laser radiation to obtain fluorescence spectra for study the spectroscopic properties of ICG NPs colloidal solution with 0.25·μM concentration (Fig. 5a).

During the exposion to a sample of ICG NPs colloidal solution by laser radiation with wavelengths of 750 and 800 nm, an intense fluorescence peak corresponding to ICG NPs J-aggregates was observed. When the sample is excited with 650 and 700 nm wavelengths, in addition to fluorescence of J-aggregates, a small fluorescence peak corresponding to ICG monomers is observed at 815 nm. It was noted that with an increase of laser radiation wavelength, a shift of the fluorescence peak to the short-wavelength region is observed, at the same time the dependence of the fluorescence peak and the wavelength is linear.

Fig. 5b shows the dependence of the fluorescent signal intensity (displayed in color) on the excitation wavelength for ICG NPs colloidal solution. The maximum fluorescence intensity of ICG NPs J-aggregates is observed with laser radiation with wavelengths in the range of 775-800 nm. There is also a fluorescence shift in of ICG NPs J-aggregates to the short-wave region with an increase in the wavelength of laser radiation (for clarification, a vertical dashed line at 900 nm wavelength is drawn).

In the course of the work, the J-aggregates fluorescence signal of ICG NPs colloidal solution under resonant excitation was also studied. A sample with a ICG NPs colloidal solution with a 0.25 μM concentration was irradiated with different wavelengths in 880-915 nm range. Polylatex calibration spheres with 110 nm diameter were used as a reference sample to obtain the instrument response function of the assembled system and assess polarizer system imperfections. The spectra of scattered laser radiation on samples of ICG NPs colloidal solution and calibration spheres in 880-915 nm wavelength range with 1 nm adjustment tuning step were obtained (Fig.6). The dependences of the intensity maxima of radiation

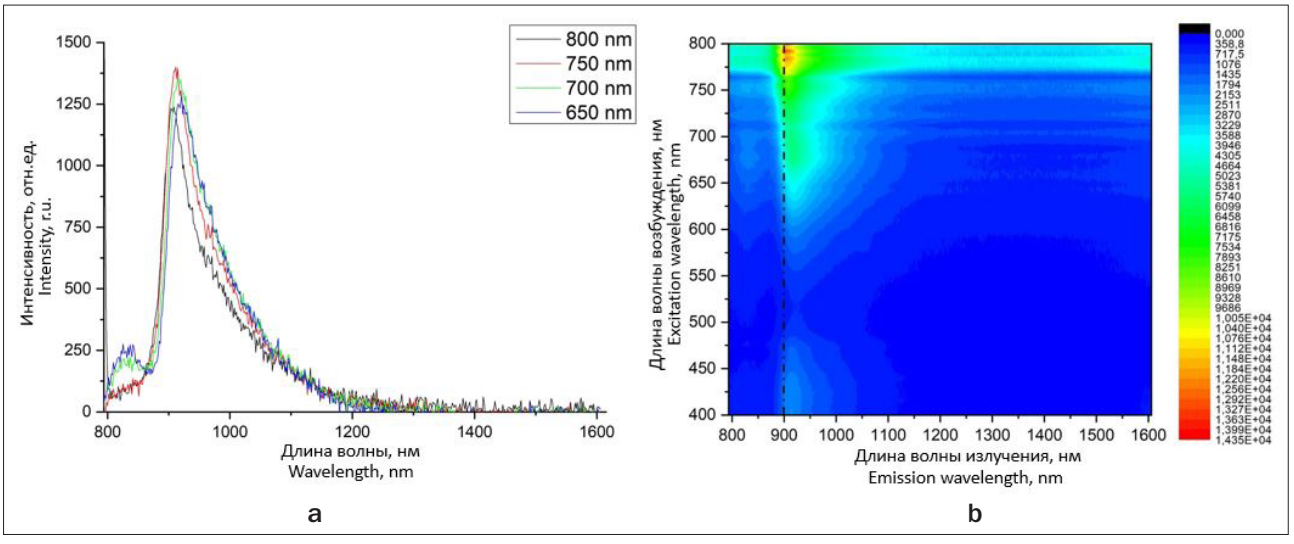

Рис. 5.
a – спектры флуоресценции J-агрегатов коллоидного раствора ICG NPs при возбуждении на 650, 700, 750 и 800 нм;
b – спектральная карта флуоресценции нормированных интенсивностей испускания флуоресценции при различных длинах волн.
Fig. 5.
a – fluorescence spectra of J-aggregates of ICG NPs colloidal solution at 650, 700, 750 and 800 nm excitation;
b – spectral map of normalized fluorescence emission intensities at different wavelengths.

scattered on samples of ICG NPs colloidal solution and calibration spheres were obtained for visual observation of changes in the intensity of scattered laser radiation (Fig.7a).

The decrease of the laser light scattered by the sample is observed with an increase of the laser radiation wavelength (Fig. 7a). The intensity maxima ratio of the scattered laser radiation from ICG NPs sample to a calibration sphere sample was obtained for evaluation of the spectroscopic properties of the ICG NPs colloidal solution (Fig. 7b). This dependence demonstrates the ability of ICG NPs colloidal solution to absorb in 893-896 nm range. Fig. 8 shows the ratio of the intensity maxima values of the scattered laser signal on ICG NPs colloidal solution to the calibration sphere sample, which shows the absorption caused by J-aggregates. To confirm this effect, absorption spectra were obtained via a two-

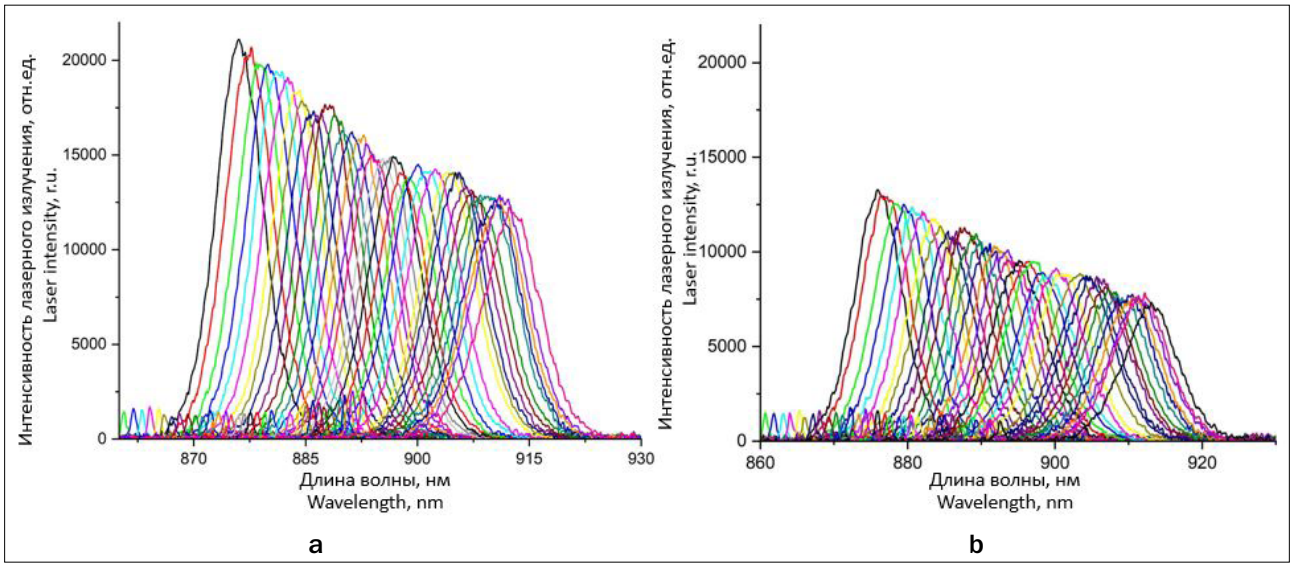

Рис. 6. Спектры рассеянного лазерного излучения, прошедшего через образец под 90°:
a – ICG NPs; b – калибровочные сферы
Fig.6. Spectra of scattered laser radiation transmitted through the sample at 90°:
a – ICG NPs; b – calibration spheres

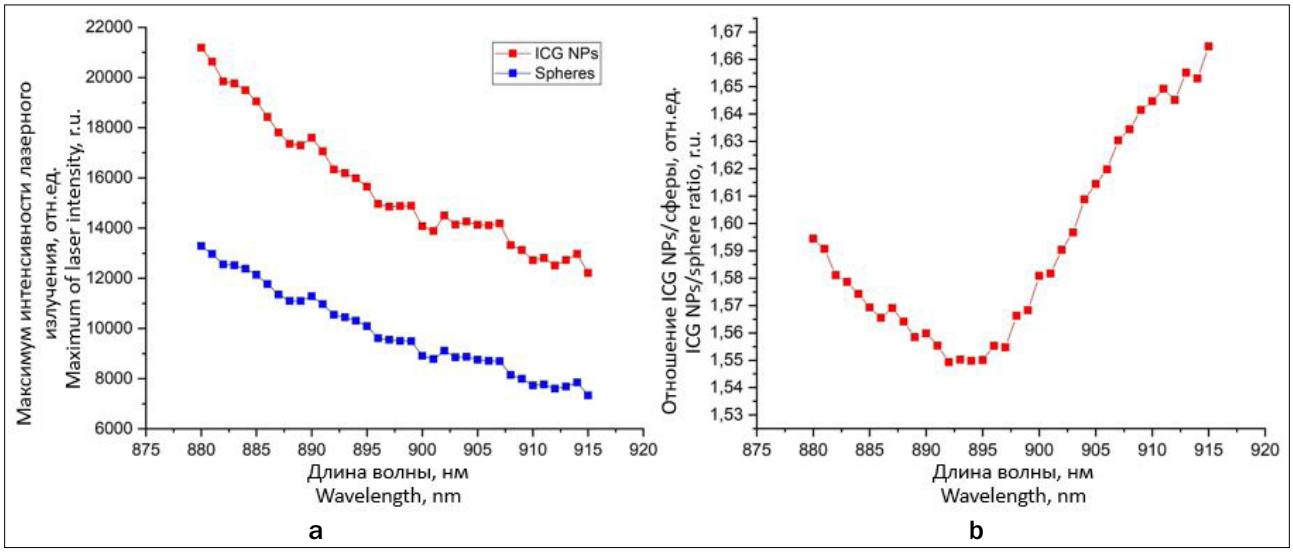

Рис. 7.
a – максимумы интенсивностей рассеянного излучения, прошедшего через образцы ICG NPs и калибровочные сферы в зависимости от длины волны лазерного излучения;
b – отношение максимумов интенсивностей рассеянного лазерного излучения, прошедшего через образец ICG NPs к калибровочным сферам.
Fig. 7.
a – intensity maxima of the radiation scattered by ICG NPs and calibration spheres depending on the laser radiation wavelength;
b – the ratio of the intensity maxima of the laser radiation scattered by ICG NPs sample to the calibration sphere sample.

beam spectrophotometer and a spectrometer when light passes through the sample to the lumen from a broadband source through ICG NPs colloidal solution and calibration spheres at 180°angle (Fig. 8).

According to the data obtained by two different methods, the J-aggregate maximum absorption of the ICG NPs colloidal solution is observed at 893 nm wavelength (Fig. 8).

To suppress the intensity of the laser radiation signal, a 880/10 nm cleaning narrowband filter was installed in front of the sample. Also, the spectra of the laser signal scattered on the samples were obtained with the configuration of the installation at 90° angle (Fig. 9).

Fig. 10a shows that a decrease in the maximum intensities of the scattered laser signal occurs with an increase in the wavelength of the laser radiation, while after 892 nm a low signal of scattered radiation is observed, which indicates the absorption of the laser signal by a narrow-band filter. The ratio of the intensity maxima of the scattered laser signal in Fig. 10b shows a decrease in the dependence values due to the absorption of J-aggregates of the ICG NPs colloidal solution and subsequent absorption by a narrowband filter of 880/10 nm.

The absorption spectra of J-aggregates when heating ICG NPs colloidal solution to a temperature of 65°C were used to plot a graph on a double logarithmic scale in order to estimate the aggregate number of nanoparticles [12]. From this dependence, based on the law of mass action:

$$K = \frac{C_{agg}}{C_m^n} \tag{5}$$

$$C_0 = C_m + nC_{agg} \tag{6}$$

$$C_0 - C_m = nC_{agg} = nKC_m^n \tag{7}$$

$$\lg nC_{agg} = \lg nK + n \lg C_m \tag{8}$$

where n – the monomer number forming the aggregate, K – proportionality coefficient, C_0 – total concentration of fluorescent dye, C_m – concentration of monomer ICG, C_{agg} – J-aggregate concentration. According to these equations, an aggregate number of ICG molecules was obtained equal to 4, which demonstrate spectroscopic properties corresponding to ICG NPs J-aggregates (Fig. 11). This result is confirmed by studies of the concentration dependences of the spectroscopic effect in work [13], assuming thermodynamic equilibrium between two ICG states: a monomer solution and J-aggregates. The aggregate number of molecules for H-aggregates of ICG is 2.

For obtaining a scattering indicatrix of light transmitted through samples of ICG NPs colloidal solution and calibration spheres, the installation shown in Fig. 3 was assembled with 920 nm wavelength. The data of the angular dependence of light scattering characterize the scattering properties of the object by their appearance, which allows comparing the shape and size of J-aggregates of ICG NPs colloidal solution with calibration spheres. Polar diagrams of the intensity dependence of scattered laser light on the rotation angle of the receiving fiber were obtained (Fig. 12).

The obtained data of polar diagrams of the light scattering indicatrix transmitted through a colloidal solution and calibration spheres are shown in Fig. 12, and demonstrate the change in the intensity of scattered light from the scattering angle. The scattering indicatrix of the light transmitted through the calibration spheres

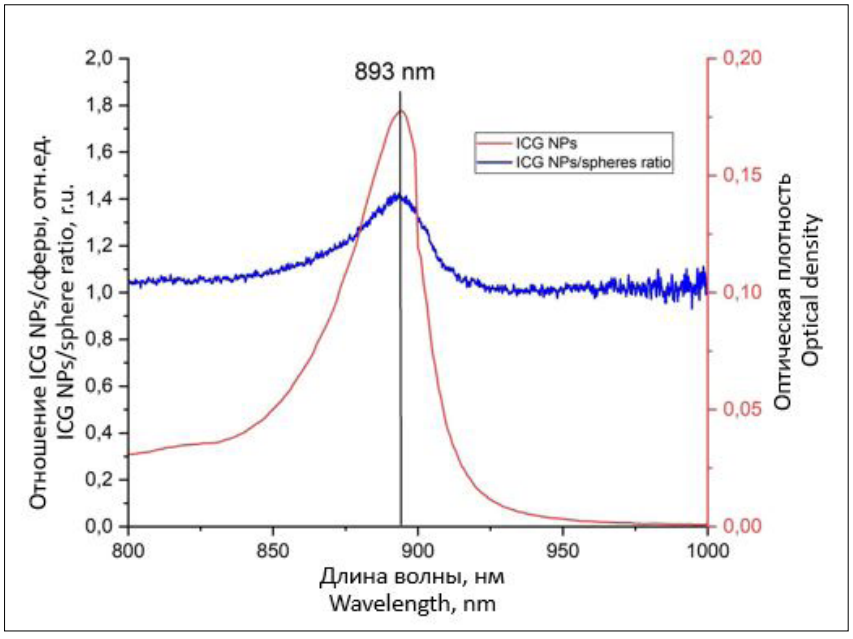

Рис. 8. Отношение спектров пропускания света через коллоидный раствор ICG NPs и через калибровочные сферы, полученных при помощи широкополосного источника света и волоконного спектрометра (синяя линия), спектр поглощения коллоидного раствора ICG NPs, полученный при помощи двухлучевого спектрофотометра (красная линия).
Fig. 8. The ratio of the light transmission spectra through the ICG NPs colloidal solution and the calibration spheres obtained via a broadband light source and a fiber spectrometer (blue line), the absorption spectrum of the ICG NPs colloidal solution obtained via a two-beam spectrophotometer (red line).

have a more elongated shape, which shows a cosine close to the one unit of the scattering angle compared to the ICG NPs colloidal solution. The calculated value of the g-factor according to the Henyey-Greenstein formula with 920 nm wavelength for the ICG NPs colloidal solution was 0.76, while for calibration spheres it was 0.86.

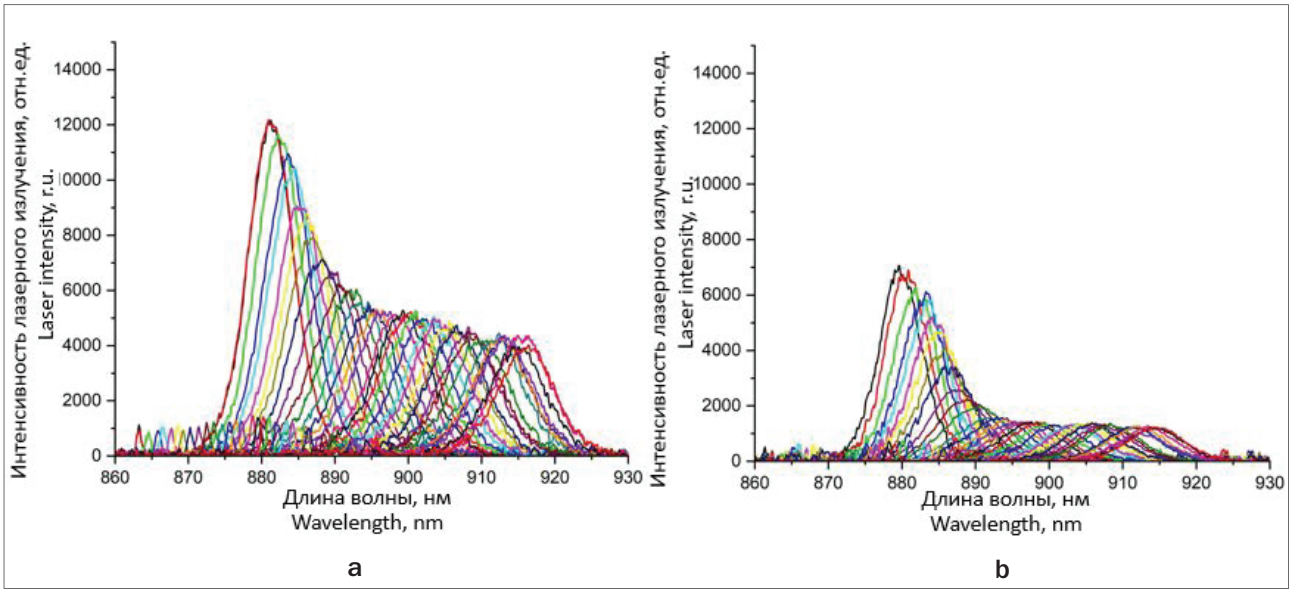

Рис. 9. Полученные спектры лазерного излучения, рассеянного на образцах под углом 90° с узкополосным фильтром 880/10 нм:
a – ICG NPs;
b – калибровочные сферы.
Fig. 9. The obtained spectra of laser radiation scattered on samples at 90° angle with 880/10 nm narrow-band filter:
a – ICG NPs;
b – calibration spheres.

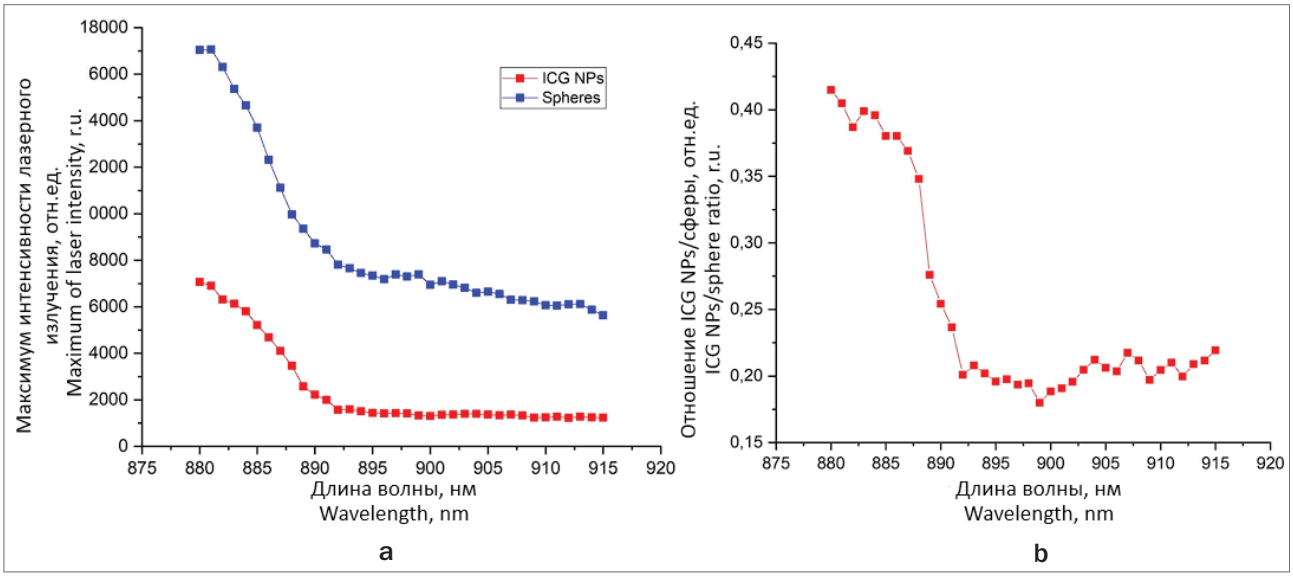

Рис. 10.
a – максимумы интенсивностей рассеянного лазерного излучения на образцах ICG NPs и на калибровочных сферах в зависимости от длины волны лазерного излучения;
b – отношение максимумов интенсивностей рассеянного лазерного излучения на образце ICG NPs и на калибровочных сферах.
Fig. 10.
a – intensity maxima of scattered laser radiation on samples of ICG NPs and the calibration spheres depending on the laser radiation wavelength;
b – the intensity maxim ratio of scattered laser radiation on the sample of ICG NPs and the calibration spheres.

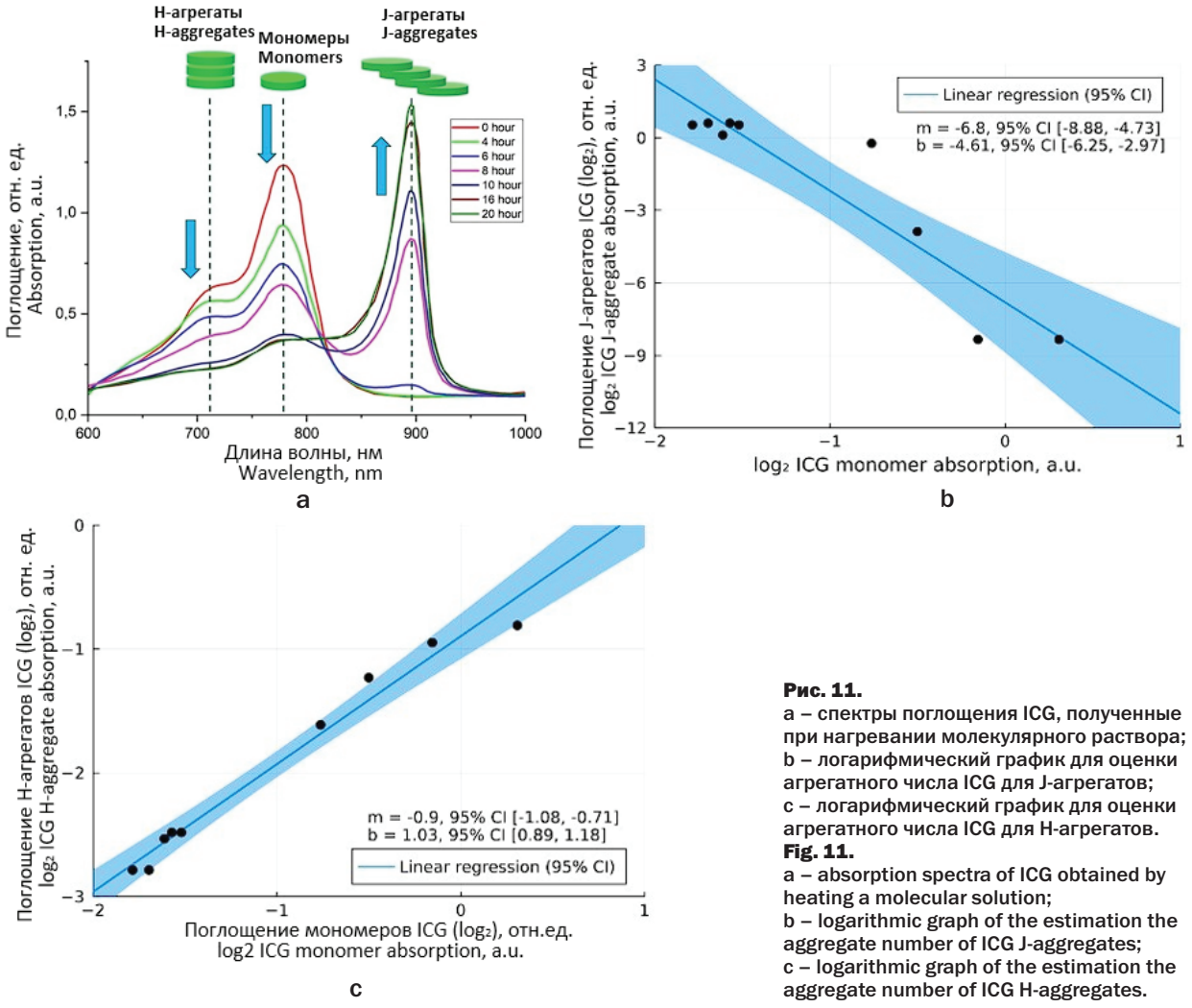

Рис. 11.
a – спектры поглощения ICG, полученные при нагревании молекулярного раствора;
b – логарифмический график для оценки агрегатного числа ICG для J-агрегатов;
c – логарифмический график для оценки агрегатного числа ICG для H-агрегатов.
Fig. 11.
a – absorption spectra of ICG obtained by heating a molecular solution;
b – logarithmic graph of the estimation the aggregate number of ICG J-aggregates;
c – logarithmic graph of the estimation the aggregate number of ICG H-aggregates.

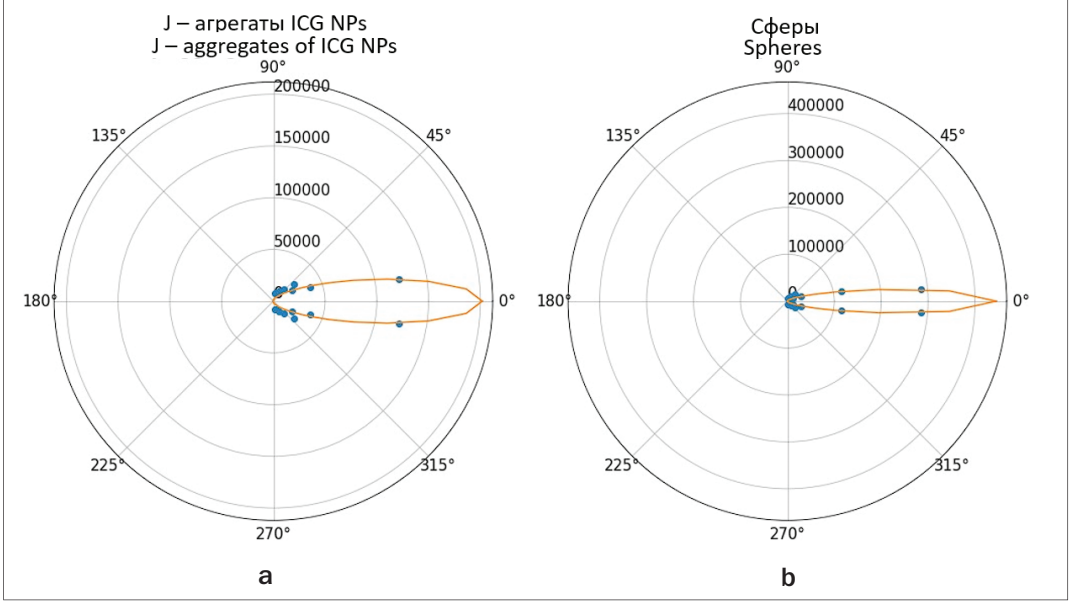

Рис. 12. Индикатрисы рассеяния света образцами:
a – коллоидный раствор ICG NPs;
b – калибровочные сферы.
Fig. 12. The scattering indicatrix of the by the samples:
a – ICG NPs colloidal solution;
b – calibration spheres.

For estimation the average size and aggregation degree of the J-aggregates of ICG NPs colloidal solution at different concentrations, the scattered light intensities on nanoparticles at 15° and 145° angles were measured by the Mie scattering method. On the basis of these data, the differential cross-sections of the Mie scattering are calculated as presented in study [11]. The experimentally obtained differential cross-sections of Mie scattering at θ = 15° and θ = 145° allowed us to determine the average aggregation degree and the average size of the J-aggregates of ICG NPs colloidal solution, respectively (Fig. 13a).

The aggregation degree of nanoparticles increases from 1.25×10^9 for 2·μM to 2.38×10^9 for 0.5 mM concentration of ICG NPs colloidal solution. Absorption spectra of ICG NPs colloidal solution were obtained from which the absorption coefficient of J-aggregates was calculated. Fig. 10b shows how the absorption coefficient of J-aggregates decreases with increasing concentrations, while the average size of J-aggregates increases, which varies from 144 nm for 2·μM to 175 nm for 0.5 mM concentration of ICG NPs colloidal solution. Presumably, until 75 μM, ICG NPs J-aggregates grow vertically by adding ICG molecules above and below by non–covalent π-π stacking, while after 75 μM, they increase in width by growing sideways and/or forming other ICG NPs J-aggregates.

Images of J-aggregates of ICG NPs colloidal solution were obtained by SEM method to study the morphological structure (Fig. 14).

Microscopic images show the position of ICG NPs J-aggregates in the form of large sheet-like conglomerates and in the form of flakes consisting of granular material, and with a wide size distribution. The J-aggregates of the ICG NPs colloidal solution are a tightly packed network of long rod-shaped conglomerates in the obtained images. Based on the obtained images, it is impossible to determine individual J-aggregates from beginning to end and the intersection points between individual aggregates, at the same time the J-aggregates are slightly curved. The formation of a network is the cause of the strong viscoelasticity observed in solutions. According to the obtained images, ICG NPs J-aggregates with 5·μM concentration are about 100-110 nm wide of the sheet-like aggregate and, presumably, more than 1 μm in length (Fig. 14a). With the concentration increase of the ICG

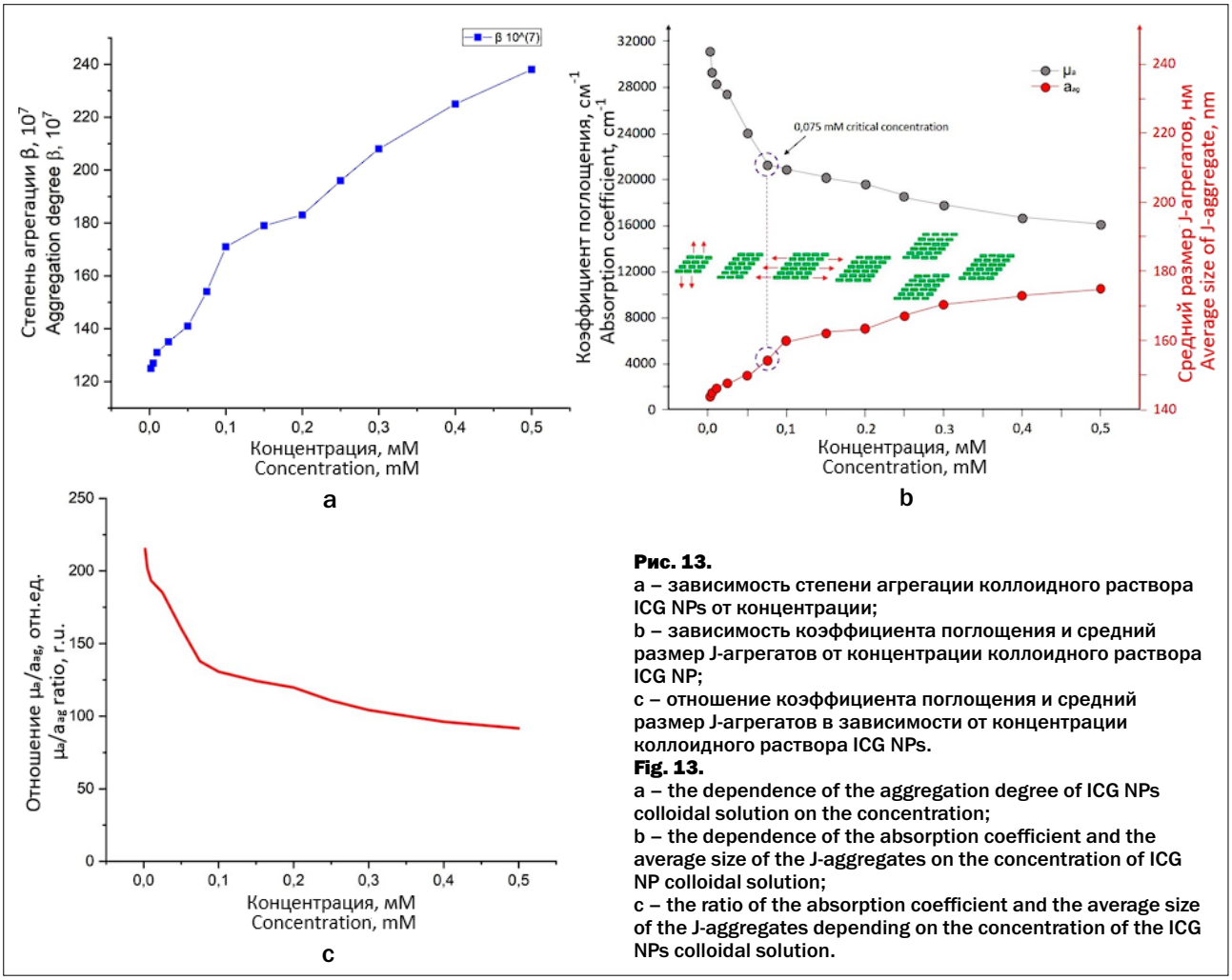

Рис. 13.
a – зависимость степени агрегации коллоидного раствора ICG NPs от концентрации;
b – зависимость коэффициента поглощения и средний размер J-агрегатов от концентрации коллоидного раствора ICG NP;
c – отношение коэффициента поглощения и средний размер J-агрегатов в зависимости от концентрации коллоидного раствора ICG NPs.

Fig. 13.
a – the dependence of the aggregation degree of ICG NPs colloidal solution on the concentration;
b – the dependence of the absorption coefficient and the average size of the J-aggregates on the concentration of ICG NP colloidal solution;
c – the ratio of the absorption coefficient and the average size of the J-aggregates depending on the concentration of the ICG NPs colloidal solution.

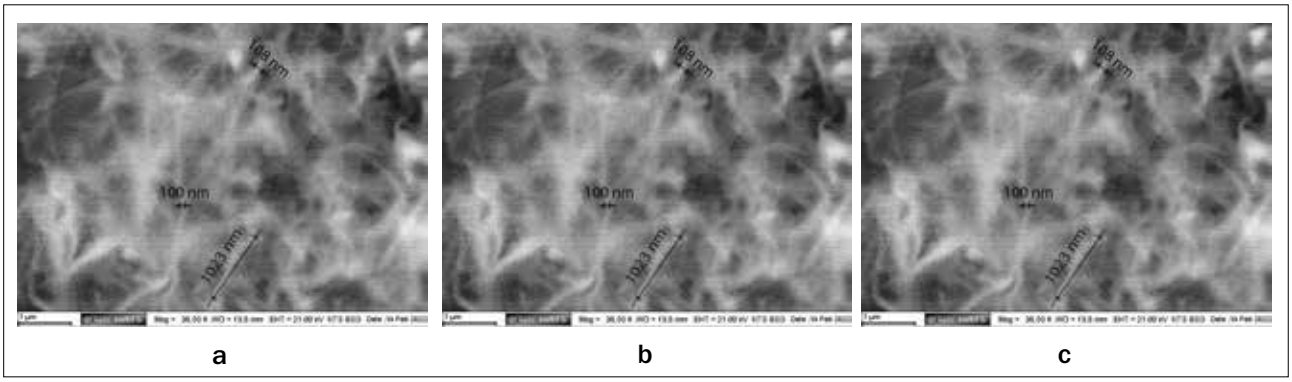

Рис. 14. SEM изображения J-агрегатов ICG NPs с концентрациями:
a – 5 μM; b – 0.1 мМ; c – 0.5 мМ.
Fig. 14. SEM images of ICG NPs J-aggregates with concentrations:
a – 5 μM; b – 0.1 mM; c – 0.5 mM.

NPs colloidal solution to 0.1 mM, the dimensions of the aggregates increase to 120 ± 5 nm in width and 1050 ± 15 nm in length (Fig. 14b). For higher concentrations than 0.5 mM, J-aggregates are large particles with a width up to 500 nm and a length up to 1 μm (Fig. 14c).

Discussion

In this work, the spectroscopic properties of ICG NPs colloidal solution, which mainly consists of J-aggregates were considered. A shift of the fluorescence maximum of ICG NPs J-aggregates to the short-wavelength range is noted with an increase in the wavelength of laser radiation. The spectral map of fluorescence upon excitation with different wavelengths of laser radiation demonstrates the broadening of the emission spectrum of ICG NPs J-aggregates with increasing fluorescence intensity.

During the study of scattered laser radiation on ICG NPs colloidal solution passing through crossed linear polarizers, a laser radiation signal was observed. The resonant fluorescence of ICG NPs colloidal solution turned out to be less intense compared to the scattered laser radiation, and the quality of the polarizer and the analyzer system did not allow to register a fluorescent signal.

Spectroscopic methods were used to obtain the minimum number of ICG molecules lined up in the brickwork of the ICG NPs J-aggregate, equal to 4, for the bathochromic shift of the optical properties of ICG NPs colloidal solution. When exposed to electromagnetic radiation, the upper and lower molecules rise on one side, breaking the bonds of interaction between the molecules (Fig. 15). The proposed configuration of molecules in the ICG NPs J-aggregate is potentially consistent with the data obtained from the law of mass action (Eq. 5-8).

Scattered laser radiation was recorded on a J-aggregates sample of ICG NPs colloidal solution by transverse scanning with a receiving fiber at different scattering angles to study the scattering indicatrix. It was noted that the efficiency of the scattered laser signal increases with decreasing scattering angle. The scattering indicatrix of light passing through the ICG NPs colloidal solution has an elongated forward shape, which is confirmed by the anisotropy g-factor calculated using the Henyey-Greenstein formula, equal to 0.76.

The aggregation degree and the average size of J-aggregates were investigated with increasing concentration of ICG NPs colloidal solution. The scattered signal at an 15° angle provided information on the average aggregation degree of the nanoparticles, while the scattered signal at an 145° angle provided information of the J-aggregates average size. A polydisperse size distribution of aggregates was noted, with increasing concentration increasing the J-aggregate size of ICG NPs and their aggregation degree, while the absorption coefficient decreases, which is consistent with theoretical studies [15]. The decrease in the absorption coefficient of J-aggregates is caused by a decrease in the total specific surface of molecules with an increase in their size [16, 17]. ICG monomers are added mainly from above and below the J-aggregate and slowly across up to a critical colloidal solution concentration of 75 μM. After that, J-aggregates begin to slowly build monomers in height and contribute to the addition of ICG molecules on the sides and/or form new J-aggregates.

In SEM images, ICG NPs J-aggregates are densely packed molecules with a sheet-like morphology, which is consistent with the brickwork packing model of ICG molecules proposed by Kuhn et al [18]. At the same time, with an increase in the concentration of the ICG NPs colloidal solution, a change in the structural morphology of the J-aggregate occurs, which is demonstrated by the addition of ICG monomers to the surface of the aggregates.

Based on the obtained data, a new model of the structural arrangement of molecules in the ICG J-aggregate under the action of laser radiation was proposed. The angle between the transition dipoles and the molecular axis of the aggregate determines whether the transition

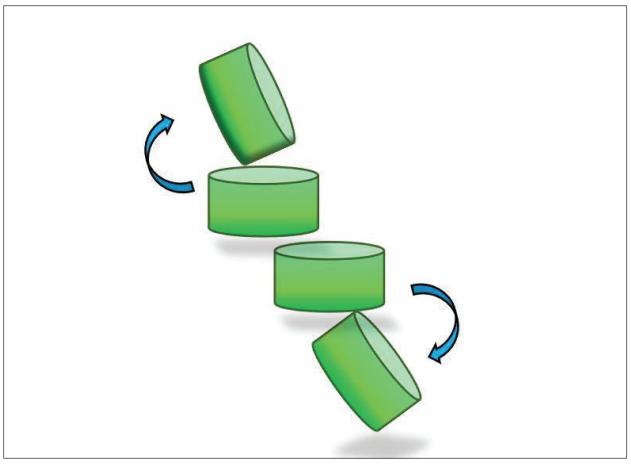

Рис. 15. Схематическое изображение активации молекул в J-агрегате ICG NPs при воздействии лазерного излучения.
Fig. 15. Schematic representation of the activation of molecules in the ICG NPs J-aggregate under the laser radiation.

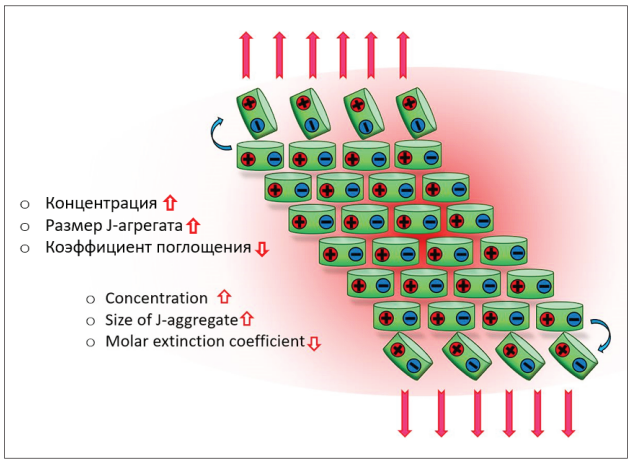

Рис. 16. Структурное расположение молекул в J-агрегате ICG NPs при воздействии лазерного излучения.
Fig. 16. Structural arrangement of molecules in the ICG NPs J-aggregate under the laser radiation.

to lower or higher levels of the excited state is allowed. In J- and H-type ICG aggregates, the excited state splits into two nondegenerate states. The low energy state is formed in the J-type ICG, which corresponds to codirectionally oriented transition dipole moments, while the high state contains transition dipoles with opposite orientations. In J-aggregates, only transitions to the lower level of the split excited state, which corresponds to the bathochromic spectral shift, are possible. J-aggregates of ICG NPs colloidal solution are arranged in monomolecular layers of molecules, the long axes of which lie parallel to the plane of the layer (Fig. 16). The shift of the absorption peak to the long wavelength region of the J-aggregate is due to the large lateral shift along the long molecular axis between adjacent ICG monomers. The dipole moments of the electronic transitions of individual molecules in the aggregate are aligned parallel to the line connecting their centers through the head-tail arrangement of the monomers. When exposed to electromagnetic radiation in this configuration, interactions occur with molecules located on the surface of the J-aggregate, which rise, breaking one interaction bond with the molecules of the aggregate with a greatly increased dipole moment (Fig. 16).

Resonant excitation occurs on the surface molecules of the J-aggregate. The narrow fluorescence spectrum is justified by the simultaneous uplift of molecules on the surface of the aggregate. As the concentration increases, a quasi-two-dimensional superstructure of ICG monomers occurs on the surface of the J-aggregate. The decrease in the absorption coefficient with increasing concentration is characterized by an increase in the probability of molecules transition to an excited state due to an increase in the number of molecules that make up ICG NPs J-aggregate. At the same time, J-aggregates are characterized by a wide size distribution, which varies from small oligomer particles to sheet-like aggregates hundreds of nanometers long.

Conclusion

This paper presents the optical characteristics of ICG NPs colloidal solution, mainly consisting of J-aggregates. The obtained scattering indicatrix and anisotropy factor give an idea of the size of the ICG aggregate shape. According to the obtained characteristics by Mie scattering methods, a change in spectral characteristics was noted with an increase in the concentration of ICG NPs colloidal solution. The aggregation degree and the average size of the J-aggregates of ICG NPs colloidal solution increases with increasing concentration, while the absorption coefficient decreases, which is associated with a decrease in the specific surface area with an increase in the size of the J-aggregates. The SEM study showed a sheet-like morphology of J-aggregates with subsequent attachment of ICG monomers to the surface of the aggregate with increasing concentration. Based on the obtained data, a behavior model of ICG monomers that are part of the J-aggregate was formulated. The upper and lower molecules located on the domain are able to move from para-position to ortho-position, demonstrating fluorescent properties with a greatly increased oscillator strength, which is associated with an increase in the radiation velocity. The use of ICG NPs colloidal solution in clinical practice will improve the efficiency of fluorescent diagnostics of tumor tissue, the boundaries of its growth and the pathways of metastasis.

Acknowledgment

The reported study was funded by RFBR according to the research project No. 21-52-15025 and partly by IEA (International Emerging Action) CNRS grant 00534.

REFERENCES

1. Shakiba M., Ng K.K., Huynh E., Chan H., Charron D.M., Chen J., Muhanna N., Foster F.S., Wilson B.C. and Zheng G. Stable J-aggregation enabled dual photoacoustic and fluorescence nanoparticles for intraoperative cancer imaging // Nanoscale. – 2016. – 8. – P.12618-12625. https://doi.org/10.1039/C5NR08165C
2. Zweck J. and Penzkofer A. Microstructure of indocyanine green J-aggregates in aqueous solution // Chemical Physics. – 20010. – 269. P.399-409. https://doi.org/10.1016/S0301-0104(01)00368-8
3. Bricks J.L., Slominskii Y.L., Panas I.D. and Demchenko A.P. Fluorescent J-aggregates of cyanine dyes: basic research and applications review // Methods and applications in fluorescence. – 2017. – 6, P.012001.
4. Obara Y., Saitoh K., Oda M. and Tani T. Room-temperature fluorescence lifetime of pseudoisocyanine (PIC) J excitons with various aggregate morphologies in relation to microcavity polariton formation // International Journal of Molecular Sciences. -2012. – 13. P.5851-5865. https://doi.org/10.3390/ijms13055851
5. Hill T.K., Abdulahad A., Kelkar S.S., Marini F.C., Long T.E., Provenzale J.M. and Mohs A.M. Indocyanine green-loaded nanoparticles for image-guided tumor surgery // Bioconjugate chemistry. – 2015. – 26. P.294-303. https://doi.org/10.1021/bc5005679
6. Wittmann M., Rotermund F., Weigand R. and Penzkofer A. Saturable absorption and absorption recovery of indocyanine green J-aggregates in water // Applied Physics B: Lasers &Optics. – 1998. – 66.
7. Würthner F., Kaiser T.E. and Saha-Möller C.R. J-aggregates: from serendipitous discovery to supramolecular engineering of functional dye materials // Angew. Chem., Int. Ed. – 2011. -50. P.3376–410. https://doi.org/10.1002/anie.201002307
8. Farrakhova D., Maklygina Y., Romanishkin I., Yakovlev D., Plyutinskaya A., Bezdetnaya L. and Loschenov V. Fluorescence imaging analysis of distribution of indocyanine green in molecular and nanoform in tumor model // Photodiagnosis and Photodynamic Therapy. – 2022. – 37. P.102636. https://doi.org/10.1016/j.pdpdt.2021.102636
9. Farrakhova D., Romanishkin I., Maklygina Y., Bezdetnaya L. and Loschenov V. Analysis of Fluorescence Decay Kinetics of Indocyanine Green Monomers and Aggregates in Brain Tumor Model In Vivo // Nanomaterials. – 2021. – 11, P.3185. https://doi.org/10.3390/nano11123185
10. Farrakhova D.S., Romanishkin I.D., Yakovlev D.V., Maklygina Yu.S., Savelieva T.A., Bezdetnaya L., Loschenov V.B. The spectroscopic study of indocyanine green J-aggregate stability in human blood and plasma // Physics of Wave Phenomena. – 2022. – 30. P.86-90. https://doi.org/10.3103/S1541308X22020029
11. Weigand R., Rotermund F. and Penzkofer A. Degree of aggregation of indocyanine green in aqueous solutions determined by Mie scattering // Chemical physics. – 1997. – 220. 373-P.384. https://doi.org/10.1016/S0301-0104(97)00150-X
12. Liu R., Tang J., Xu Y., Zhou Y., Dai Z. Nano-sized indocyanine green J-aggregate as a one-component theranostic agent // Nanotheranostics. – 2017. – 1. P.430. https://doi.org/10.7150/ntno.19935
13. Wang J., Pang X., Tan X., Song Y., Liu L., You Q., Sun Q., Tan F., Li N. A triple-synergistic strategy for combinational photo/radiotherapy and multi-modality imaging based on hyaluronic acid-hybridized polyaniline-coated WS2 nanodots // Nanoscale. – 2017. – 9. P.5551-5564. https://doi.org/10.1039/C6NR09219E
14. Berlepsch H.V. and Böttcher C. Cryo-transmission electron microscopy reveals mesoscopic H-and J-aggregates of near infrared cyanine dyes // Journal of Photochemistry and Photobiology A: Chemistry. – 2010. -214. P.16-21. https://doi.org/10.1016/j.jphotochem.2010.05.025
15. Weigand R., Rotermund F. and Penzkofer A. Aggregation dependent absorption reduction of indocyanine green // The Journal of Physical Chemistry A. – 1997. – 101. P.7729-7734. https://doi.org/10.1021/jp9700894
16. Gregg S.D. and Sing K.S.W. Adsorption, Surface Area and Porosity // Journal of The electrochemical society. – 1967. – 114. P.279Ca.
17. Lowell S. and Shields J. E. Powder surface area and porosity // Springer Science & Business Media. – 1991. – 2.
18. Czikkely V., Försterling H.D. and Kuhn H. Light absorption and structure of aggregates of dye molecules // Chem. Phys. Lett. – 1970. – 6. P.11–14. https://doi.org/10.1016/0009-2614(70)80062-8

ЛИТЕРАТУРА

1. Shakiba M., Ng K.K., Huynh E., Chan H., Charron D.M., Chen J., Muhanna N., Foster F.S., Wilson B.C. and Zheng G. Stable J-aggregation enabled dual photoacoustic and fluorescence nanoparticles for intraoperative cancer imaging // Nanoscale. – 2016. – 8. – P.12618-12625. https://doi.org/10.1039/C5NR08165C
2. Zweck J. and Penzkofer A. Microstructure of indocyanine green J-aggregates in aqueous solution // Chemical Physics. – 2001. – 269. P.399-409. https://doi.org/10.1016/S0301-0104(01)00368-8
3. Bricks J.L., Slominskii Y.L., Panas I.D. and Demchenko A.P. Fluorescent J-aggregates of cyanine dyes: basic research and applications review // Methods and applications in fluorescence. – 2017. – 6, P.012001.
4. Obara Y., Saitoh K., Oda M. and Tani T. Room-temperature fluorescence lifetime of pseudoisocyanine (PIC) J excitons with various aggregate morphologies in relation to microcavity polariton formation // International Journal of Molecular Sciences. -2012. – 13. P.5851-5865. https://doi.org/10.3390/ijms13055851
5. Hill T.K., Abdulahad A., Kelkar S.S., Marini F.C., Long T.E., Provenzale J.M. and Mohs A.M. Indocyanine green-loaded nanoparticles for image-guided tumor surgery // Bioconjugate chemistry. – 2015. – 26. P.294-303. https://doi.org/10.1021/bc5005679
6. Wittmann M., Rotermund F., Weigand R. and Penzkofer A. Saturable absorption and absorption recovery of indocyanine green J-aggregates in water // Applied Physics B: Lasers &Optics. – 1998. – 66.
7. Würthner F., Kaiser T.E. and Saha-Möller C.R. J-aggregates: from serendipitous discovery to supramolecular engineering of functional dye materials // Angew. Chem., Int. Ed. – 2011. -50. P.3376–410. https://doi.org/10.1002/anie.201002307
8. Farrakhova D., Maklygina Y., Romanishkin I., Yakovlev D., Plyutinskaya A., Bezdetnaya L. and Loschenov V. Fluorescence imaging analysis of distribution of indocyanine green in molecular and nanoform in tumor model // Photodiagnosis and Photodynamic Therapy. – 2022. – 37. P.102636. https://doi.org/10.1016/j.pdpdt.2021.102636
9. Farrakhova D., Romanishkin I., Maklygina Y., Bezdetnaya L. and Loschenov V. Analysis of Fluorescence Decay Kinetics of Indocyanine Green Monomers and Aggregates in Brain Tumor Model In Vivo // Nanomaterials. – 2021. – 11, P.3185. https://doi.org/10.3390/nano11123185
10. Farrakhova D.S., Romanishkin I.D., Yakovlev D.V., Maklygina Yu.S., Savelieva T.A., Bezdetnaya L., Loschenov V.B. The spectroscopic study of indocyanine green J-aggregate stability in human blood and plasma // Physics of Wave Phenomena. – 2022. – 30. P.86-90. https://doi.org/10.3103/S1541308X22020029
11. Weigand R., Rotermund F. and Penzkofer A. Degree of aggregation of indocyanine green in aqueous solutions determined by Mie scattering // Chemical physics. – 1997. – 220. 373-P.384. https://doi.org/10.1016/S0301-0104(97)00150-X
12. Liu R., Tang J., Xu Y., Zhou Y., Dai Z. Nano-sized indocyanine green J-aggregate as a one-component theranostic agent // Nanotheranostics. – 2017. – 1. P.430. https://doi.org/10.7150/ntno.19935
13. Wang J., Pang X., Tan X., Song Y., Liu L., You Q., Sun Q., Tan F., Li N. A triple-synergistic strategy for combinational photo/radiotherapy and multi-modality imaging based on hyaluronic acid-hybridized polyaniline-coated WS2 nanodots // Nanoscale. – 2017. – 9. P.5551-5564. https://doi.org/10.1039/C6NR09219E
14. Berlepsch H.V. and Böttcher C. Cryo-transmission electron microscopy reveals mesoscopic H-and J-aggregates of near infrared cyanine dyes // Journal of Photochemistry and Photobiology A: Chemistry. – 2010. -214. P.16-21. https://doi.org/10.1016/j.jphotochem.2010.05.025
15. Weigand R., Rotermund F. and Penzkofer A. Aggregation dependent absorption reduction of indocyanine green // The Journal of Physical Chemistry A. – 1997. – 101. P.7729-7734. https://doi.org/10.1021/jp9700894
16. Gregg S.D. and Sing K.S.W. Adsorption, Surface Area and Porosity // Journal of The electrochemical society. – 1967. – 114. P.279Ca.
17. Lowell S. and Shields J. E. Powder surface area and porosity // Springer Science & Business Media. – 1991. – 2.
18. Czikkely V., Försterling H.D. and Kuhn H. Light absorption and structure of aggregates of dye molecules // Chem. Phys. Lett. – 1970. – 6. P.11–14. https://doi.org/10.1016/0009-2614(70)80062-8